Agricultural and Forest Meteorology 303 (2021) 108385

Contents lists available at ScienceDirect

Agricultural and Forest Meteorology

journal homepage: www.elsevier.com/locate/agrformet

Discrepant responses between evapotranspiration- and transpiration-based ecosystem water use efficiency to interannual precipitation fluctuations

Chunjie Gu [a], Qiuhong Tang [a,b,*], Gaofeng Zhu [c], Jinzhu Ma [c], Chunli Gu [d], Kun Zhang [e], Shuang Sun [f], Qiang Yu [g], Shuli Niu [b,h]

[a] Key Laboratory of Water Cycle and Related Land Surface Processes, Institute of Geographic Sciences and Natural Resources Research, Chinese Academy of Sciences, Beijing 100101, China
[b] University of Chinese Academy of Sciences, Beijing 100094, China
[c] Key Laboratory of Western China's Environmental Systems (Ministry of Education), College of Earth and Environmental Sciences, Lanzhou University, Lanzhou, China
[d] Beijing Institute of Applied Meteorology, Beijing 100029, China
[e] National Tibetan Plateau Data Center, Institute of Tibetan Plateau Research, Chinese Academy of Sciences, Beijing 100101, China
[f] State Key Laboratory of Earth Surface Processes and Resource Ecology, Faculty of Geographical Science, Beijing Normal University, Beijing 100875, China
[g] State Key Laboratory of Soil Erosion and Dryland Farming on the Loess Plateau, Northwest A&F University, Yangling 712100, Shaanxi, China
[h] Key Laboratory of Ecosystem Network Observation and Modeling, Institute of Geographic Sciences and Natural Resources Research, Chinese Academy of Sciences, Beijing, China

ARTICLE INFO

Keywords:
Ecosystem water use efficiency
Eddy covariance
PT-JPL model
PM model
Precipitation fluctuations
Evapotranspiration partition
Water availability

ABSTRACT

Climate change intensifies precipitation fluctuation and increases drought frequency around the globe. Water use efficiency (WUE) has proven to be a crucial metric to quantify the trade-off linking global carbon and water cycles in many aspects of terrestrial ecosystem function. Investigating the response of ecosystem WUE to multiannual precipitation fluctuations has major implications for our understanding of ecosystem carbon and water dynamics. However, the impacts of water availability variation on evapotranspiration- and transpiration-based ecosystem WUE and their mechanisms are poorly understood due to limited observations. We investigated ecosystem WUE in response to interannual precipitation fluctuations in order to reveal the regularity underlying WUE changes under different levels of water stress. We optimized the parameters of two remote sensing models (PT-JPL and PM) based on different biophysical processes using the differential-evolution Markov Chain (DE-MC) method. We investigated ecosystem WUE_{ET} (GPP/ET) and WUE_T (GPP/T) in response to interannual precipitation fluctuations at 73 sites. We found ecosystem WUE_T appears to decline during drought years and to increase in wet years contrasting with WUE_{ET}, which was mostly attributable to differing sensitivities of GPP, ET and T to multiannual precipitation fluctuations. The vegetation generally consumes more T to improve ecosystem GPP during dry years, meanwhile, no apparent change in WUE_{ET} during dry years because of the trade of between GPP/T and T/ET. The replenishment of soil moisture to ecosystem transpiration is higher than we thought during dry years. This was masked in analysis that considered the responses of GPP and T to annual precipitation changes separately, but was revealed by the changes in ecosystem WUE_T. This research advances our understanding of the consequences of water fluctuation on ecosystem carbon and water exchange.

1. Introduction

Carbon and water cycles are intimately coupled in terrestrial ecosystems. Water-use-efficiency (WUE), the proportion of carbon assimilation per unit of water loss, has been recognized as an important indicator of the relationship between the water and carbon cycles and is a key characteristic of ecosystem function (Ponton et al., 2006; Keenan et al., 2013). Global climate change is likely to shift precipitation patterns and cause the frequency and intensity of droughts to increase, which will affect ecosystem carbon and water processes (Dai 2013; Yin et al., 2016; Berdugo et al., 2020). Interannual variability of precipitation can influence the components of the hydrological budget and alter net CO_2 uptake from the atmosphere (Tang et al., 2011; Carvalhais et al., 2014). This can affect ecosystem function within terrestrial biomes

* Corresponding author.
E-mail address: tangqh@igsnrr.ac.cn (Q. Tang).

https://doi.org/10.1016/j.agrformet.2021.108385
Received 3 April 2020; Received in revised form 13 February 2021; Accepted 28 February 2021
0168-1923/© 2021 Elsevier B.V. All rights reserved.

through adjustments in vegetation structure and function (Easterling et al. 2000; Fatichi & Ivanov, 2014). Meanwhile, the response of terrestrial ecosystems to changes in water availability is one of the greatest challenges associated with climate change (Brooks et al., 2011). WUE is an important consideration when simulating primary productivity in models. The carbon sink is dominated by ecosystem productivity whose carbon balance is strongly associated with precipitation. Changes in WUE in wet and dry years is directly related to the trend and inter annual variability of the carbon sink (Ahlström et al., 2015). Therefore, an understanding of ecosystem WUE and its key controlling processes in response to precipitation fluctuations is helpful to project terrestrial carbon feedbacks caused by climate change.

WUE is an important consideration when simulating primary productivity in models. Therefore, an understanding of ecosystem WUE and its key controlling processes in response to precipitation fluctuations is helpful to project terrestrial carbon feedbacks caused by climate change. Definitions for WUE metrics range in spatial scale from leaf to ecosystem, and range in temporal scale from instantaneous measurements to multi-year ecosystem life cycles (Beer et al., 2009; Bernacchi and VanLoocke 2015; Tarin et al., 2019). The diversity of definitions for WUE is caused by multiple ways of quantifying carbon exchange and water loss (Potts et al., 2006; Li et al., 2010; Peñuelas et al., 2011). The most widely used ecosystem WUE metric is defined as the ratio between GPP and ET (Ito and Inatomi., 2012; Liu et al., 2020). This focuses on the direct exchange of carbon and water gross fluxes between ecosystem and the atmosphere, Another common metric is intrinsic WUE,the ratio of Gross Primary Productivity (GPP) to canopy conductance. Intrinsic WUE is defined as the ratio of carbon assimilation (A) to stomatal conductance (g_s) at the leaf scale, and is commonly used to study the effects of rising atmospheric CO_2 concentration on plant physiology (Keenan et al., 2013; Peters et al.,2018; Knauer et al., 2018). The different ways of measuring ecosystem WUE involve different eco-physiological processes, which makes them difficult to compare, and leads to a divergence in understanding the mechanisms causing variability in ecosystem WUE.

The response of ecosystem WUE_{ET} (defined as GPP/ET) to water availability varies considerably between studies. Reichstei et al. (2002) analyzed three Mediterranean ecosystems using eddy covariance and sapflow data and found ecosystem WUE_{ET} decreases during drought. They also studied the effect of the 2003 heat wave on the productivity of the European biosphere in summer, observing a slight decrease in WUE_{ET} despite a strong negative anomaly of GPP during the severe drought (Reichstein et al., 2007). Hu et al. (2008) quantified the inter-annual variations of WUE_{ET} along a water availability gradient at four Chinese grassland locations and found a positive correlation with precipitation. Lu and Zhang (2010) derived WUE_{ET} on a continental scale and found that WUE_{ET} tended to increase under moderate drought conditions but tended to decrease under seveer drought conditions. Niu et al. (2011) found that increased precipitation stimulated WUE_{ET} at temperate steppe in Northern China.

These inconsistent responses of ecosystem WUE_{ET} to precipitation can be explained in part by different study periods, types of vegetation or other confounding factors that may have been ignored (Yu et al., 2008; Ponce Campos et al., 2013). However, the coupling of ecosystem carbon and water exchange processes and its key controlling processes in response to precipitation variation are still unclear. Given that ET includes soil evaporation (ES), canopy interception (EI) and transpiration (T), trends in non-biological processes such as EI and ES may also contribute to the response of WUE_{ET}. WUE_T represents ecosystem-level carbon assimilation associated with physiologically water loss and is defined as defined as GPP divided by T (Hu et al., 2008; Sun et al., 2015). WUE_T represents a strictly-defined process of carbon and water exchange with stomata regulating the movement of water vapor from vegetation into the atmosphere and CO_2 from the atmosphere into vegetation. Studies of WUE_T are relatively rare due to the difficulty in observing transpiration and simulating inaccurate (Lian et al.,2015; Zhang et al.,2016). The response of WUE_T to precipitation changes is therefore not well understood. It is currently unclear how different measures of ecosystem WUE capture variation with changes of annual precipitation (Tarin et al., 2019).

Our current understanding of the effect of multiannual precipitation variability on ecosystem WUE is still poor due to sparse and scattered *in-situ* data. It is impossible to further study whether there are some commonalities internal mechanisms among different ecosystem to adjust the response of WUE to annual precipitation. Here we compare the responses of annual WUE_{ET} and WUE_T to changes in annual precipitation at the site-level to record ecosystem resilience under disturbances of water and maintain ecosystem functions. Specifically, the questions we address are: (i) what are the magnitudes of variability for WUE_{ET} and WUE_T across different biomes within different climate zones? (ii) How do WUE_{ET} and WUE_T respond to precipitation fluctuation at the stand-level? (iii) What are the mechanisms underlying the different responses of ecosystem WUE_{ET} and WUE_T to annual precipitation changes?

2. Materials and methods

2.1. Forcing data

2.1.1. Tower data selection

FLUXNET is a global network of continuous eddy covariance measurements of carbon dioxide, water vapor and energy exchange on half-hourly to annual timescales between the biosphere and atmosphere (Baldocchi et al., 2014, 2003; Barr et al., 2006). This standardized dataset allows us to analyze many sites across diverse environmental conditions. Direct measurements of carbon and water exchange make it possible to evaluate ecosystem WUE and to investigate the responses to environmental change at the ecosystem level (Huxman et al., 2004; Law et al., 2002). Here we use the FLUXNET2015 dataset which includes several improvements to enhance data quality from multiple regional flux networks. In order to analyze the influence of annual precipitation change on WUE, 73 sites were selected based on the the screening criteria which required more than five years of observational data available since 2000 (Figure S1). With a combined 678 site-years of measurements the data coverage at each site ranges from 5 to 14 years across a wide range of vegetation classes, including croplands (CRO; 13 sites), deciduous broadleaf forests (DBF; 12 sites), evergreen broadleaf forests (EBF; 6 sites), evergreen needleleaf forests (ENF; 18 sites), grasslands (GRA; 10 sites), mixed forests (MF; 6 sites), open shrublands (OSH; 3 sites), savannas (SAV; 2 sites), and woody savannas (WAS; 3 sites). A more detailed description of the 73 sites is provided in Supplemental Table S1 and at www.fluxdata.org.

2.1.2. Energy budget closure

A discrepancy of 10∼30% in the surface energy balance is generally observed when calculating the difference between net radiation and the sum of the latent, sensible and soil heat fluxes at eddy covariance towers. This is a universal problem and is not due to the uncertainty in observations alone. The best way to correct the non-closure problem is still under discussion (Massman and Lee, 2002; Barr et al., 2006; Foken et al., 2011). The values of the latent and sensible heat fluxes were corrected by the closure ratio in the FLUXNET2015 dataset. Here we use the latent heat flux data after this correction to optimize the model parameters.

2.1.3. Remote sensing data

Remote sensing data are required for the ET model inputs including the enhanced vegetation index (*EVI*), the normalized difference vegetation index (*NDVI*) and the leaf area index (*LAI*). The values were acquired from moderate-resolution imaging spectroradiometer (MODIS) products at 1km spatial resolution around the eddy covariance flux sites with high quality-controlled (Myneni et al., 2002). We used linear interpolation to fill gaps between successive satellite data records, and then integrated the indexes to a monthly scale.

2.2. Remote sensing model and ET partition

2.2.1. PT-JPL model

The Priestly-Taylor Jet Propulsion Laboratory (PT-JPL) model uses a number of biophysical constraints to downscale potential *ET*. It relies on the Priestley-Taylor equation to calculate veritable *ET*, which was proposed by Fisher et al. (2008). The PT-JPL model has been widely used in *ET* evaluation for its superior performance when compared to other remote sense *ET* models across multiple flux towers (Ershadi et al., 2014; Michel et al., 2016; McCabe et al. 2016). The model is governed by the following equations:

$$ET = T + ES + EI \tag{1}$$

$$T = (1 - f_{wet}) f_g f_T f_M \cdot \alpha \frac{\Delta}{\Delta + \gamma} \cdot R_{nc} \tag{2}$$

$$ES = (f_{wet} + f_{sm}(1 - f_{wet})) \cdot \alpha \frac{\Delta}{\Delta + \gamma} \cdot (R_{ns} - G) \tag{3}$$

$$EI = f_{wet} \cdot \alpha \frac{\Delta}{\Delta + \gamma} \cdot R_{nc} \tag{4}$$

where R_{nc} is the canopy net radiation (W/m^2), R_{ns} is the net radiation at the soil surface (W/m^2), G is the soil heat flux (W/m^2), Δ is the slope of the saturated vapor-pressure curve (Pa/K), γ is the psychrometric constant (~0.066kPa/C), and α is an empirical multiplier constant (i.e. 1.26) (Priestley and Taylor 1972). f_{wet} is relative surface wetness (equal to the fourth power of relative humidity, RH^4), f_g is green canopy fraction, f_T is plant temperature constraint, f_M is plant moisture constraint, f_{SM} is soil moisture constraint. The weighting functions are defined as:

$$f_g = f_{APAR} / f_{IPAR} \tag{5}$$

$$f_T = \exp\left[\left(- - \frac{T_a - - T_{opt}}{T_{opt}} \right)^2\right] \tag{6}$$

$$f_M = f_{APAR} / f_{APARmax} \tag{7}$$

$$f_{SM} = RH^{\left(\frac{VPD}{\beta}\right)} \tag{8}$$

Where f_{APAR} and f_{IPAR} are the fractions of the photosynthesis active radiation (*PAR*) that is absorbed (*APAR*) and intercepted (*IPAR*), respectively, by vegetation cover. These values are defined as f_{APAR}=m$_1$*EVI*+b$_1$ and f_{IPAR} =m$_2$*NDVI*+b$_2$. *NDVI* is the normalized difference vegetation index, *EVI* is the enhanced vegetation index and m_1, b_1, m_2 and b_2 are parameters. *RH* is the relative humidity (%), *Ta* is the mean air temperature (°C), T_{opt} is the optimum temperature for plant growth (°C), *VPD* is the saturation vapor pressure deficit (kPa), β is the sensitivity for soil moisture constraint to *VPD* (kPa).

2.2.2. PM model

The Penman–Monteith model (PM) incorporates mass transfer of heat and water vapour . The Penman equation (Penman, 1948) was developed to asses potential evaporation from open water and saturated land surfaces, but was later modified by Monteith (1965) with the introduction of a canopy resistance term to describe the actual evapotranspiration. The actual evaporation is given by the sum of plant transpiration (T), soil evaporation (ES) and wet canopy evaporation (EI) individually. The soil moisture constraints, aerodynamic resistance and canopy surface resistance are estimated from semi-empirical equations with different types of land cover (Cleugh et al., 2007; Mu et al., 2007, 2011). The driving equations in the model are given as

$$ET = T + ES + EI \tag{9}$$

$$T = \frac{\left(\Delta R_{nc} + \frac{\rho C_P f_c VPD}{r_a}\right) \cdot \frac{(1 - f_{wet})}{\lambda}}{\Delta + \gamma \cdot (1 + r_s)/r_a} \tag{10}$$

$$ES = \frac{\left(\Delta R_{ns} + \frac{\rho C_P (1 - f_c) VPD}{r_{as}}\right) \cdot \frac{(f_{wet} + (1 - f_{wet}) f_{sm})}{\lambda}}{\Delta + \gamma \cdot r_{tot}/r_{as}} \tag{11}$$

$$EI = \frac{\left(\Delta R_{nc} + \frac{\rho C_P f_c VPD}{r_{hrc}}\right) \cdot \frac{f_{wet}}{\lambda}}{\Delta + (P_a C_P r_{vc})/\lambda \cdot \varepsilon \cdot r_{hrc}} \tag{12}$$

where R_{nc}, R_{ns}, Δ, γ and *VPD* represent the same quantities as above. ρ is the air density (kg/m^3) ,C_p is the specific heat capacity of air (MJ/kgC), P_a is the atmospheric pressure (kPa), λ is the latent heat of evaporation (MJ/kg), ε is the ratio of the molecular weight of water to dry air (~0.622). f_c is the fractional vegetation cover, f_{wet} is the relative surface wetness and f_{sm} is the constraint to soil evaporation. these three fractional quantities are are dimensionless. r_a is the aerodynamic resistance between the mean canopy height and the air, r_s is the canopy surface resistance, r_{tot} is the total aerodynamic resistance, r_{as} is the aerodynamic resistance at the soil surface, r_{hrc} is the aerodynamic resistance on the wet canopy surface, r_{vc} is the surface resistance on the wet canopy surface, r_{hc} is the wet canopy resistance to sensible heat. The specific calculations for the resistances can be found in Mu et al. (2007, 2011) and Zhang et al. (2018).

2.2.3. Parameter optimization and ET partition

A combination of hydrometric and isotopic methods are typically used to quantify the components of ET. However, these methods are restricted by high experimental costs and relatively short observation periods. Based on remote sensing data and climatological parameters ET models provide an efficient way to calculate the components of ET, especially at broad scales or over long time periods. However, the reliability of these models is limited by the large number of parameters. Ensuring the reliability of the simulations is one of the important steps to applying the ET model application at stand-level. To this end, a number of steps were taken to improve the accuracy of the ET simulations and components. First, A global sensitivity analysis was used to calculate sensitivity parameters models. This followed the methods established by Sobol (1990, 2001). this method is based on variance decomposition and is a useful for exploring the significance of model parameters and for optimizing them (Nossent et al., 2011; Zhu et al., 2016; Zhang et al., 2017). Second, the proper posterior distributions of each key parameter were obtained using differential-evolution Markov Chain (DE-MC) estimation. These parameters were evaluated by comparing them to flux tower observations. The monthly sums of sensible heat flux (H, W/m^2) and latent heat flux (LE, W/m^2) were used to optimize model parameters. This method has been used successfully to improve model performance across different biomes owing to many ecophysiological parameters combined in the model (Zhang et al. 2017).

Due to the limitation of observation data, we validated the ecosystem T/ET merely at daily scale in order to evaluate the performance of the two models (Figure S2). The experiment was conducted in a grapevine ecosystem during the 2017 growing seasons. The study site is located in the Nanhu Oasis of northwestern China (39°52′34″N, 94°06′19″E; 1300m a.s.l.). Details of the site, eddy covariance and sap flow measurements were provided by Wang et al. (2019). The regression between the measured and the estimated values from PT-JPL and PM model of T/ET was not statistically different from 1:1 line, with R^2 being 0.77 and 0.79, respectively.

2.3. WUE calculation

Ecosystem GPP and respiration were partitioned from net ecosystem

exchange (NEE). Based on the observed relationship between nighttime respiration and temperature, the nighttime data were applied to parameterize a respiration model that was used for the entire dataset to estimate ecosystem respiration. GPP was calculated as the difference between ecosystem respiration and the net CO_2 exchange (Reichstain et al., 2005). Here WUE_{ET} is defined as the gross CO_2 assimilation relative to evapotranspiration (i.e. GPP/ET) and WUE_T is defined as the gross CO_2 assimilation relative to water loss by transpiration (i.e. GPP/T). Annual GPP and water vapor flux values were aggregated to yearly (January 1 to December 31) values at the stand-level. We only included flux sites with for more than five years of available data since 2000. For each site, the two years with the lowest annual precipitation were used to represent drought conditions and the two years with the highest precipitation were used to represent wet conditions. The responses of ecosystem WUE to annual precipitation changes were analyzed by comparing the dry and wet years. Due to the constraints of available data, we treated wetness as a categorical variable; the relative intensity of drought or wetness was not considered.

Based on the ratio of annual potential evapotranspiration and precipitation, we divided the sites into different climate zones with different water stress according to Rockström and Karlbergs (2009). Based on the radiation estimation and combined aerodynamics method with energy balance, the Priestley and Taylor methodwas used to calculate potential evapotranspiration. The Wet Index (WI=P/PET) was used to reclassify the sites into four categories: 0.2 to 0.5, 0.50 to 0.8, 0.8 to 1.0 and greater than 1.0. Due to the previous selection criterion of more than 5 years of data at each site, there were no sites in in arid areas (WI≤0.2) in our analysis.

3. Results

3.1. WUE of different sites

The flux sites included nine biomes according to the classification of the International Geosphere-Biosphere Programme (IGBP) and span a range of climatic zones. The relationship between annual WUE_{ET}, WUE_T and mean annual precipitation (MAP) are shown in Figure S3. We found that the sites with highest WUE_{ET} and WUE_T had annual precipitation values in the range of 900-1200 mm . The value of WUE_{ET} and WUE_T across vegetation classes and climatic zones were significantly different

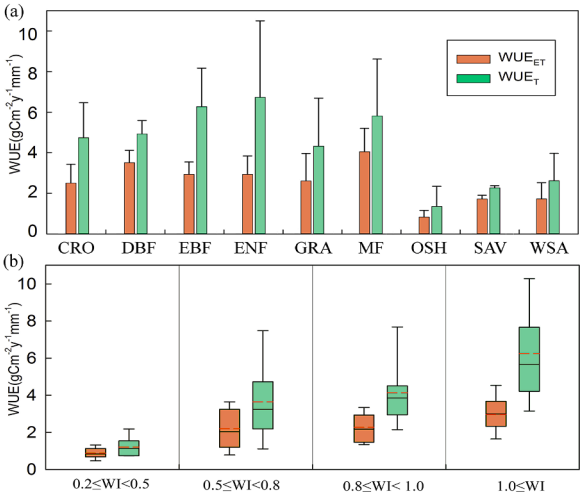

Fig. 1. The variation of stand-level WUE_{ET} and WUE_T across different biomes (a). The height of each coloured rectangle represents the median value and the top of each whisker represents one standard deviation. (b) The range of WUE_{ET} and WUE_T across different water constraints from semi-arid to humid Boxes mark the 75th and 25th percentiles and the dashed and solid lines show the average and median values, respectively.

(Fig. 1). After removing the impacts of soil evaporation and vegetation interception evaporation, WUE_T increased significantly compared with WUE_{ET}. At ENF sites for instance, the average WUE_{ET} ranged from 1.02 to 4.87 $gCm^{-2}y^{-1}$ with a median of 2.93 $gCm^{-2}y^{-1}$, whereas the average WUE_T ranged from 2.09 to 17.38 $gCm^{-2}y^{-1}$ with a median of 6.73 $gCm^{-2}y^{-1}$ (Fig. 1a). In general, the values of both WUE_{ET} and WUE_T were higher in forests (DBF, EBF, ENF and MF) than in other vegetation types. OSH had the lowest WUE_{ET} and WUE_T with the average value of 0.83 $gCm^{-2}y^{-1}$ and 1.35 $gCm^{-2}y^{-1}$, respectively. This may be related to low vegetation cover and productivity. Along a climatic gradient from semi-arid to humid zones, the average values of WUE_{ET} and WUE_T showed a gradual increase (Fig. 1b). The average WUE_{ET} and WUE_T in the semi-arid regions were 0.87 $gCm^{-2}y^{-1}$ and 1.21 $gCm^{-2}y^{-1}$, whereas in the humid regions, the average values were 3.22 $gCm^{-2}y^{-1}$ and 6.17 $gCm^{-2}y^{-1}$, respectively. As the water supply increased, the WUE of vegetation also gradually increased, due mainly to the improvement of vegetation productivity and the limited radiative evaporation in humid zones.

3.2. The influence of precipitation fluctuation on WUE

The comparison of WUE_{ET} and WUE_T between drought and wet years based on the PT-JPL model is shown in Fig. 2(a-b). The changes of WUE_{ET} in drought and wet years are relatively complex. Similarly, the changes of WUE_T show obvious variation with lower values during dry years than wet years (Fig. 2b). The ecosystem WUE_T is generally lower in dry years and higher in wet years at most sites in both water restricted and non-water restricted areas. The results from the PM model showed a similar distribution during dry and wet years (Fig. 3). The PT-JPL model has a better simulation of ET than PM model. In the following analysis, we mainly focus on the results of PT model. The statistical performance of the PT-JPL model before and after parameter optimization can be found in Table S2 within the Supplemental Information. We performed a linear regression on the annual precipitation and WUE for each site. The slope of this regression line represents the sensitivity of WUE_{ET} and WUE_T to annual precipitation. The median and average slope of this regression line for WUE_{ET} are both close to zero, while the slopes for WUE_T are both positive. This suggests that WUE_T is more sensitive than WUE_{ET} to precipitation (Fig. 2c), which means the WUE_T of ecosystem is more strongly affected by the fluctuation of annual precipitation.

For water restricted sites (WI<1), there was a more obvious reduction in GPP and ET during drought years. The GPP in semi-arid regions (dark red dots) reveals a significant increase in wet years indicating a high sensitivity of semi-arid ecosystems to variations in precipitation. The change of T in drought and wet years are contrary to GPP and ET, with more sites showing advanced trends in drought years (Fig. 4c inset histograms). It is difficult to intuitively explain the changes of GPP, ET and T in response to annual precipitation changes for all sites. Nevertheless, there are significant discrepancies between the sensitivity of WUE_{ET} and WUE_T to annual precipitation. To explore the possible explanations, we analyzed the relationship between the sensitivity of ET and T to P with the sensitivity of GPP to P as derived from the PT-JPL model (Fig. 5). The variables were normalized to eliminate the deviation caused by the quantity. The slope of each normalized variable with respect to P represents the sensitivity of that variable to annual precipitation. The normalized slopes of GPP and ET with respect to precipitation were approximately the same, which means GPP and ET have similar sensitivities to annual precipitation. However, GPP appears to be more sensitive to these fluctuations (Fig. 5a slope of the regression line 0.61<1). The relationship between the normalized sensitivity of T to P with GPP to P was less significant (Fig. 5b). Summarizing the results, we can say that the distribution of sensitivities of GPP and ET to precipitation are similar with median and mean value around 0.18 (Fig. 5c). Conversely, the distribution of sensitivities of T is significantly different as indicated by the negative median and mean values.

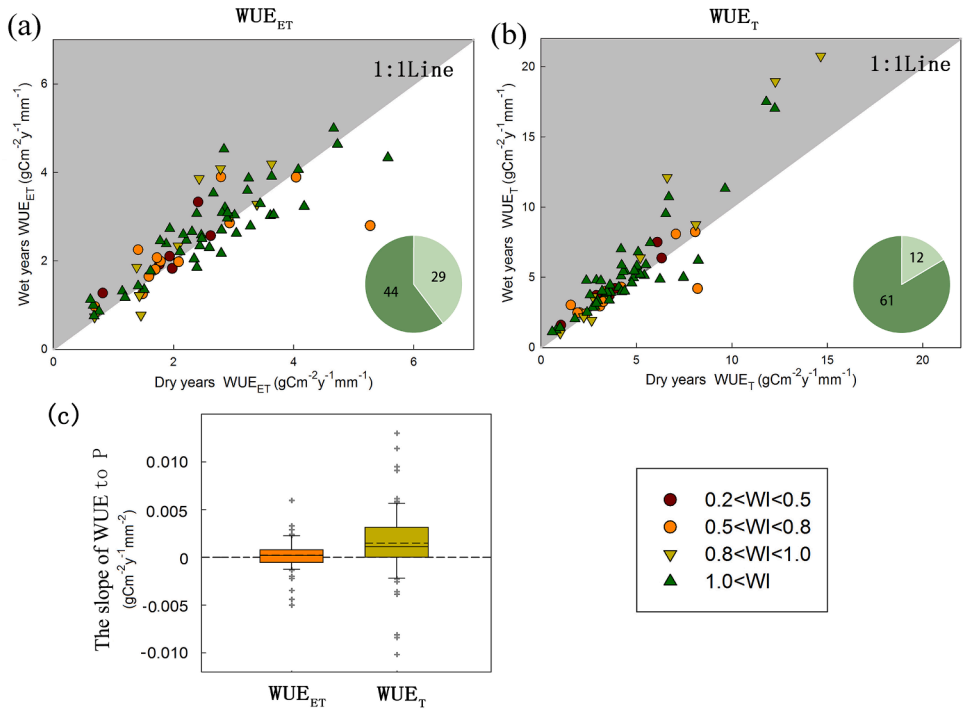

Fig. 2. Comparison of WUE_{ET} (a) and WUE_T (b) in drought and wet years. The horizontal axis is the value in dry years, and the vertical axis is the value in wet years. The results of wet years are higher in the gray area than dry year, while the results of white area are opposite. The inset pie graph summarize the total number of sites. The box plots show the slope of the regression line of WUE_{ET} or WUE_T to precipitation (c). Boxes mark the 75th and 25th percentiles and the dashed and solid lines refer to the average and median values, respectively.

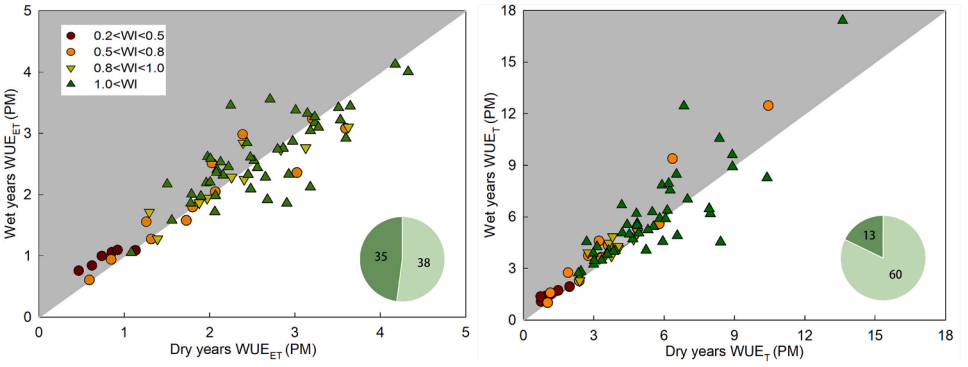

Fig. 3. Comparison of WUE_{ET}(PM) and WUE_T (PM) in drought and wet years. The horizontal axis is the value of dry years, and the vertical axis represents the result of wet years. The dots with different color represent different levels of water availability. The results of wet years are higher in the gray area than dry year, while the results of white area are opposite. The inset pie graph summarize the total number of sites with dark green represents the number of sites increased in wet years, while light green represents the number of sites decreased in wet years.

3.3. The response of ET partition to precipitation

The discrepancy between the response of ecosystem T and ET to annual precipitation fluctuations is influenced by soil evaporation (ES) and interception evaporation (EI). The fluctuation of annual precipitation also affects the segmentation of ET. The differences between T/ET, ES/ET and EI/ET ratios during drought and wet years compared to multi-year averages derived from the PT-JPL model are shown in Fig. 6. The ratio T/ET is significantly increased in drought years and was reduced in wet years (most red dots are in the upper left of the 1:1 line, and blue dots are in the lower right of the 1:1 line. Of the 73 sites, 61 increased during drought years and 57 decreased in wet years). The variations in the soil evaporation ratio ES/ET are difficult to summarize intuitively, nevertheless, more than half of the sites (51) are reduced during drought years and 46 sites are increased in wet years. The proportion of vegetation interception evaporation EI/ET showed a remarkable tendency with most sites reducing in drought years and increasing in wet years.

Overall, the segmentation of ET is affected by fluctuations of precipitation with a certain regularity. Here, the ratio T/ET decreases with increasing annual precipitation while ES/ET and EI/ET exhibit the opposite tendency. This pattern is more pronounced in trend in EI/ET than in ES/ET. During drought years, the proportion of soil evaporation and interception evaporation decreased, and more water was used to supply vegetation transpiration. However, as available water increased during wet years, the proportion of soil evaporation and the interception evaporation increased, while the proportion of transpiration decreased.

4. Discussion

4.1. Ecosystem WUE in response to precipitation fluctuations

Plants adjust physiological and structural strategies to adjust ecosystem WUE in response to different water stress (van der Molen et al., 2011). With the help of the PT-JPL and PM models, two different metrics of ecosystem water use efficiency were estimated for sites under a range of precipitation conditions. The impact of soil and interception evaporation depend on the choice of definition for ecosystem WUE. We find an obvious discrepancy between the responses of WUE_{ET} and WUE_T to annual precipitation in dry and wet years and the results are consistent between the two models. WUE_{ET} showed no obvious general pattern in response to annual precipitation, whereas WUE_T tended to be lower in dry years and greater in wet years at most sites. However, compared with the multi-year average, the value of GPP, ET and T in drought and

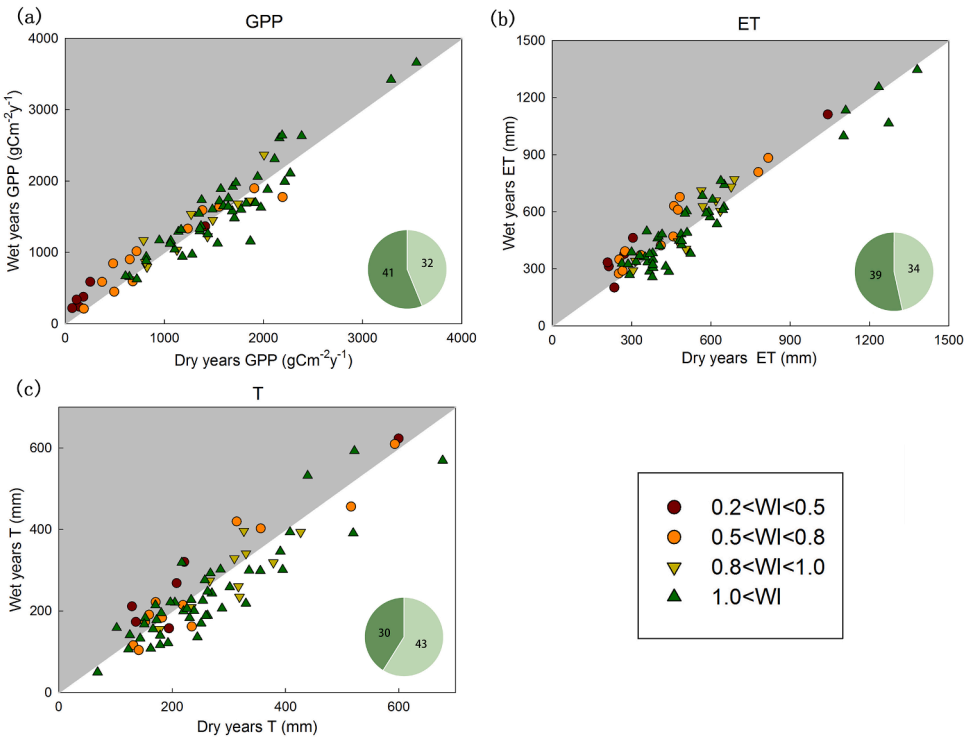

Fig. 4. Differences between GPP (a), ET (b) and T(c) in drought and wet years. The horizontal axis is the value of each parameter during dry years, and the vertical axis represents the value during wet years. The colour and shape of the dots represents different levels of water availability at the sites. The results of wet years are higher in the gray area than dry year, while the results of white area are opposite. The inset pie graph summarize the total number of sites.

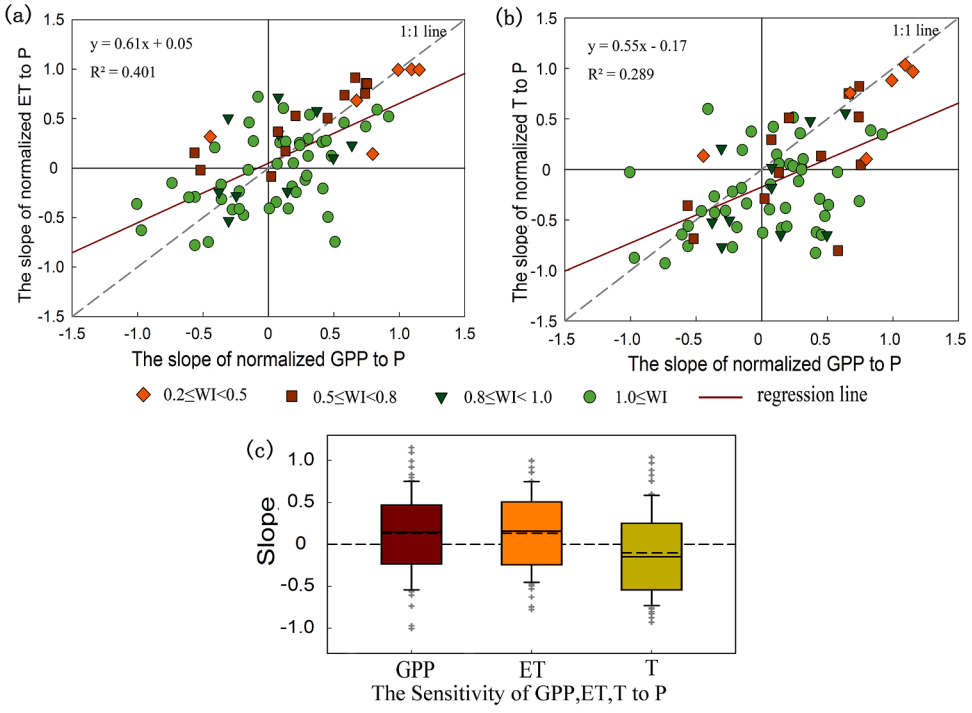

Fig. 5. The relationship between the normalized sensitivity of ET (a) and T (b) to precipitation and the normalized sensitivity of GPP to precipitation. The horizontal axis is the slope of normalized GPP to P, the vertical axis represents the slope of normalized ET to P. The dashed gray line is 1:1line and the solid red line is the regression line of all 73 sites. Diverse colors mean under different degrees of water stress. The box plots summarize the sensitivity of GPP, ET and T to annual precipitation separately (c).

wet years show no significant regularity.

We reported that decreased ecosystem WUE_T in response to decreased annual precipitation is universal for most sites over vast areas. This is consistent with other studies for specific regions. Reichstei et al. (2002) found that ecosystem WUE_T decreased during drought using eddy covariance and sapflow data in Mediterranean ecosystems. Niu et al. (2011) investigated change in WUE_T under variable precipitation in a temperate steppe and found that an increase in precipitation affected WUE_T more clearly than WUE_{ET}. This study focused on WUE in dry and wet years without considering vegetation mortality during drought and the intensity of drought and wetness.

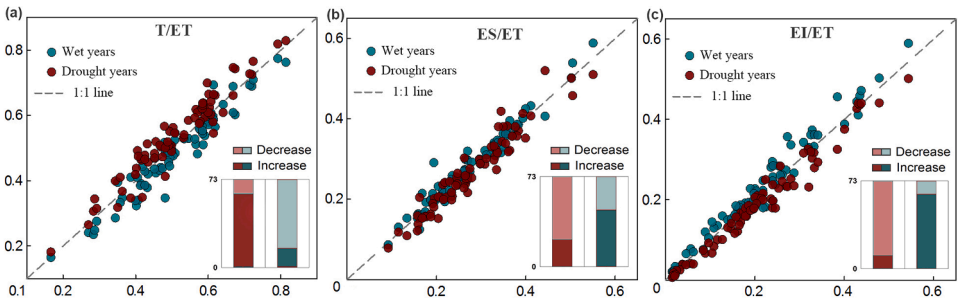

Fig. 6. Changes of T/ET (a), ES/ET (b) and EI/ET (c) in drought and wet years compared to multi-year averages. The horizontal axis is multi-year average values, and the vertical axis represents the result of the drought and wet years. The red and blue dots represent drought and wet years, respectively. The gray dashed lines are 1:1 line. The inset stacked histograms represent the numbers of sites for which the ratio decreases or increases in drought and wet years.

4.2. Explanation of divergent responses

There is a well-studied relationship between GPP, ET and precipitation based on space-for-time substitution; the consistency of ecosystem GPP and ET changes has also been discussed (Tang et al., 2006; Biederman et al., 2016; Mystakidis et al., 2016). Although there is some evidence to suggest that drought suppresses both ecosystem productivity and evapotranspiration simultaneously, the relative magnitudes vary considerably between studies (Liang et al., 2015; Beer et al., 2010). It is difficult to suggest patterns of variation for GPP, ET and T during dry and wet years due to the diverse interactions of various influences. Water and carbon cycles in ecosystems are affected by other confounding environmental factors such as temperature, solar radiation, and soil fertility. The main influencing factors in different zones are also variable (Liang et al., 2015; Engelbrecht et al., 2007). The changes in GPP, ET and T are not strictly consistent with the change in precipitation for each site in our study (Fig. 5a). Ecosystem GPP and ET have similar sensitivities to the change in annual precipitation, while the sensitivity of T to the change in annual precipitation is relatively low. The T/ET ratio decreases with an increase in annual precipitation while ES/ET and EI/ET ratios exhibit the opposite tendency at the stand-level, which means more water returns to the atmosphere through transpiration.

The lack of sensitivity of ecosystem transpiration is attributed to changes to interception evaporation and soil evaporation. The mechanisms controlling EI and ES are thought to be independent. The ratio of EI to ET is closely related to precipitation. Soil evaporation is affected by interactions between soil texture and environmental conditions with different dominant factors at the evaporation process stage (Wang et al., 2019). A decrease in precipitation leads to a decrease in soil moisture during dry years, which are often associated with higher temperatures and increased atmospheric evaporation demand. Dense vegetation can improve root capacity for soil water uptake and divert the largest part of the available soil moisture towards stomatal transpiration to enhance ecosystem GPP (Chimenti et al., 2006; Blum, 2009). For water restricted areas, we found that vegetation absorbs more water for transpiration during dry years to minimize the restriction of water on ecosystem photosynthesis and avoid a significant decrease in GPP. However, for some non-water restricted ecosystems, the vegetation generally transpires more to improve ecosystem GPP. This was hidden in the separate analysis of the responses of GPP and T to annual precipitation changes but was revealed by the changes of ecosystem WUE_T. We analyze the transpiration as a percentage of precipitation infiltrating into the soil during dry and wet years (Fig. 7). During dry years, less precipitation infiltrates into the soil before evaporative loss, but we found that the relative amount of transpiration, as a percentage of the infiltrating precipitation, actually increased. This result also supports our conclusion that plants draw water more readily from a broader range in dry years, and that the replenishment of soil moisture to ecosystem transpiration is higher than we thought.

It should be noted that we have no sites from arid zones (WI<0.2) and only six sites in semiarid zones (0.2<WI<0.5) due to of the subset of data that was selected. Regardless, there is not enough soil moisture content to provide more ecosystem transpiration during drought years in these regions which are heavily dependent on precipitation. Transpiration may decrease directly in dry years, which may also account for the significant decrease in GPP in dry years in arid- and semiarid regions (Biederman et al., 2016). We intend to analyze the response of ecosystem WUE to annual precipitation fluctuations in these areas at the global grid scale to supplement the lack of site-scale research and to verify our conclusions at other regions.

4.3. Inconsistent with leaf scale responses

There are some distinctions that should be made between the

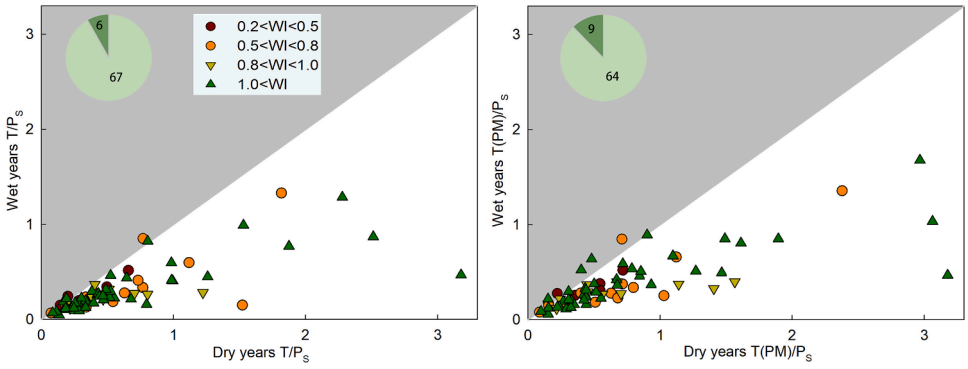

Fig. 7. Comparison of the of transpiration (from PT-JPL and PM) as a percentage of precipitation infiltrating into the soil during drought and wet years. The horizontal axis is the value during dry years, and the vertical axis is the value during wet years. The dots with different color represent different levels of water availability. The results of wet years are higher in the gray area than dry year, while the results of white area are opposite. The inset pie graph summarize the total number of sites.

response of ecosystem WUE_T and the response of leaf scale gas exchange to changes in water stress. At the leaf scale, water-use efficiency is defined as the ratio of net CO_2 assimilated by photosynthesis (A) to the water transpired (T). Leaf stomatal conductance decreases more slowly with the photosynthetic rate than with the transpiration rate under moderate water stress, which leads to the increase of WUE (Farquhar & Sharkey, 1982; Manzoni et al., 2011). Meanwhile, plants modify multiple leaf traits (i.e., narrower leaf width, increased trichome density and improved leaf reflectance) under drought conditions to increase WUE (Franks et al., 2009; Morton et al., 2014). In contrast, our results show that ecosystem WUE_T is significantly decreased at the majority of sites during drought years. Plants can make appropriate alterations in response to changing water regimes to increase their fitness. Only classical stomatal conductance could not account for the response of canopy gas exchange to water restrictions, which could be partly explained via changes in photosynthetic capacities or patchy stomatal closure (Reichstein et al., 2002, 2003).

Some studies discussed the inconsistency between instantaneous WUE at leaf scale and whole-plant scale, which may be due to the canopy leaf position and night transpiration (Poni et al., 2009; Medrano et al., 2015; Medlyn et al., 2017). Reduced annual precipitation leads to water deficit inducing nutrient deficit and imbalance which could be a mechanism for decreased plant performance and decreased WUE (McDowell et al., 2011, 2008). At stand and ecosystem levels, the response of WUE to water stress couldn't be easily scaled up from leaf scale owing to variable plant functional types with different water-use strategies and environmental conditions (Schulze et al., 1987; Niu et al.,2011; Lavergne et al., 2019). In addition to the effect of canopy complexity, the response of vegetation to precipitation fluctuation is associated with different physiological and phenological responses in plant species. Within biomes, variation in the timing and amount of precipitation may lead to changes to the dominant vegetation type and vegetation structure (Engelbrecht et al., 2007).

4.4. The uncertainty of outcome

Our results are based on the analysis of a large amount of data and models results of ecosystem T, however, the results of the models are still highly uncertain, which need to be further verified by more extensive experiments in the future. There are some other sources of uncertainty in our analysis. First, the uncertainty in the measured variables used as forcing data; the eddy covariance data are subject to scale-dependent and method-specific uncertainties (Ershadi et al., 2013). There is also a mismatch in the spatial resolution between the flux tower sites and the remotely-sensed vegetation index used in the model simulation. Second, the effect of energy balance non-closure could reduce the accuracy of WUE estimates (Knauer et al., 2018). In our study, the observed latent heat flux was used to calculate WUE_{ET}, while the site-level transpiration was obtained from parameter-optimized models using the observed data after energy closure corrections, which may affect the accuracy of the results. Finally, the greatest possible source of uncertainty may come from NEE and ET partitioning algorithm, especially current partitioning of T from ET is highly uncertain. Using the observations, we optimized model parameters and improved the simulated total ET, however, the segmentation of ecosystem ET is still difficult to verify. Among these, the EI/ET ratio showed a significant reduction during drought years and an increase during wet years, which may be related to the simple hypothesis of this part in the model. Nonetheless, considering the structure and good simulation performance of the ET model (Ershadi et al., 2014; Michel et al., 2016; McCabe et al., 2016), we still consider the simulation results to be reliable. The parameter optimization procedure and the evaluation of simulation performance for the PT-JPL model has been discussed in previous studies (Gu et al., 2018).

The selection of flux sites was limited by available data and did not include arid regions (WI < 0.2), which limits the applicability of our results to arid ecosystems. In addition to precipitation, there are many other external forcings (e.g. temperature and radiation) influencing the ecosystem carbon-water cycle process, and the key controlling factors across different regions are different (Seddon et al., 2016). Finally, our focus was on annual precipitation fluctuation and did not take into account the precipitation distribution within a year. Changes to precipitation distribution at different growth stages may affect ecosystem WUE (Sergio et al., 2013).

5. Conclusion

This study of stand-level ecosystem WUE contributes some new understanding about the response of ecosystems to climate change and provides valuable avenues for further research. In particular, we found ecosystem WUE_T appears to decline during drought years and to increase in wet years contrasting with WUE_{ET}, which was mostly attributable to differing sensitivities of GPP, ET and T to multiannual precipitation fluctuations. The vegetation generally consumes more T to improve ecosystem GPP during dry years, meanwhile, no apparent change in WUE_{ET} during dry years because of the trade of between GPP/T and T/ET. The replenishment of soil moisture to ecosystem transpiration is higher than we thought during years with little rainfall. Our study further verified the inconsistency of the response of carbon and water exchange to drought between the leaf and ecosystem scales. This research advances the understanding of the consequences of precipitation fluctuation on ecosystem carbon and water exchange, which should be included into process-based terrestrial ecosystem models to better predict the impacts of ongoing global change.

Declaration of Competing Interest

The authors declare that they have no known competing financial interests or personal relationships that could have appeared to influence the work reported in this paper.

Acknowledgements

This research was supported by the National Natural Science Foundation of China (41790424, 41730645), and International Partnership Program of Chinese Academy of Sciences (131A11KYSB20180034, 131A11KYSB20170113).

This work used eddy covariance data acquired from the FLUXNET2015 Dataset acquired and shared by the FLUXNET community, including these networks: AmeriFlux, AfriFlux, AsiaFlux, CarboAfrica, CarboEuropeIP, CarboItaly, CarboMont, ChinaFlux, Fluxnet-Canada, GreenGrass, ICOS, KoFlux, LBA, NECC, OzFlux-TERN, TCOS-Siberia, and USCCC. The ERA-Interim reanalysis data are provided by ECMWF and processed by LSCE. The FLUXNET eddy covariance data processing and harmonization was carried out by the European Fluxes Database Cluster, AmeriFlux Management Project, and Fluxdata project of FLUXNET, with the support of CDIAC and ICOS Ecosystem Thematic Center, and the OzFlux, ChinaFlux and AsiaFlux offices. MODIS NDVI, EVI, LAI satellite products were obtained online (https://modis.ornl.gov/).

Supplementary materials

Supplementary material associated with this article can be found, in the online version, at doi:10.1016/j.agrformet.2021.108385.

References

Ahlström, A., Raupach, M.R., Schurgers, G., et al., 2015. The dominant role of semi-arid ecosystems in the trend and variability of the land CO2 sink. Science 348, 895–899.

Barr, A.G., Morgenstern, K., Black, T.A., McCaughey, J.H., Nesic, Z., 2006. Surface energy balance closure by the eddy-covariance method above three boreal forest stands and implications for the measurement of the CO_2 flux. Agric. For. Meteorol. 140 (1–4), 322–337.

Beer, C., Ciais, P., Reichstein, M., Baldocchi, D., Law, B.E., Papale, D., Wohlfahrt, G., 2009. Temporal and among-site variability of inherent water use efficiency at the ecosystem level. Global Biogeochem. Cycles 23, GB2018.
Beer, C., Reichstein, M., Tomelleri, E., Ciais, P., Jung, M., Carvalhais, N., Papalel, D., 2010. Terrestrial gross carbon dioxide uptake: global distribution and covariation with climate. Science 329, 834–838.
Berdugo, M., Delgado-Baquerizo, M, Soliveres, S., Hernández-Clemente, R., Zhao, Y., Maestre, F.T., 2020. Global ecosystem thresholds driven by aridity. Science 367, 787–790.
Bernacchi, C.J., VanLoocke, A., 2015. Terrestrial Ecosystems in a Changing Environment: A Dominant Role for Water. Ann. Rev. Plant Biol. Vol. 66, 599–622.
Biederman, J.A., Scott, R.L., Goulden, M.L., Vargas, R., Litvak, M.E., Kolb, T.E., Burns, S. P., 2016. Terrestrial carbon balance in a drier world: the effects of water availability in southwestern North America. Glob. Change Biol. 22, 1867–1879.
Blum, A., 2009. Effective use of water (EUW) and not water-use efficiency (WUE) is the target of crop yield improvement under drought stress. Field Crops Res 112, 119–123.
Brooks, P.D., Troch, P.A., Durcik, M., Gallo, E., Schlegel, M., 2011. Quantifying regional scale ecosystem response to changes in precipitation: Not all rain is created equal. Water Resour. Res. 47, W00J08.
Carvalhais, N., Forkel, M., Khomik, M., Bellarby, J., Jung, M., Migliavacca, M., Reichstein, M., 2014. Global covariation of carbon turnover times with climate in terrestrial ecosystems. Nature 514, 213–217.
Chimenti, C.A., Marcantonio, M., Hall, A.J., 2006. Divergent selection for osmotic adjustment results in improved drought tolerance in maize (Zeamays L.) in both early growth and flowering phases. Field Crops Res 95, 305–315.
Dai, A., 2013. Increasing drought under global warming in observations and models. Nat. Clim. Change 3, 52–58.
Easterling, D.R., Meehl, G.A., Parmesan, C., Changnon, S.A., Karl, T.R., Mearns, L.O., 2000. Climate extremes: observations, modeling, and impacts. Science 289, 2068–2074.
Engelbrecht, B.M.J., Comita, L.S., Condit, R., Kursar, T.A., Tyree, M.T., Turner, B.L., Hubbell, S.P, 2007. Drought sensitivity shapes species distribution patterns in tropical forests. Nature 447, 80–82.
Ershadi, A., McCabe, M.F., Evans, J.P., Chaney, N.W., Wood, E.F., 2014. Multi-site evaluation of terrestrial evaporation models using FLUXNET data. Agric. For. Meteorol. 187, 46–61.
Ershadi, A., McCabe, M.F., Evans, J.P., Walker, J.P., 2013. Effects of spatial aggregation on the multi-scale estimation of evapotranspiration. Remote Sens. Environ. 131, 51–62.
Farquhar, G., Sharkey, T., 1982. Stomatal conductance and photosynthesis. Ann. Rev. Plant Physiol. 33, 317–345.
Fatichi, S., Ivanov, V.Y., 2014. Interannual variability of evapotranspiration and vegetation productivity. Water Resour. Res. 50, 3275–3294.
Fisher, J.B., Tu, K.P., Baldocchi, D.D., 2008. Global estimates of the land-atmosphere water flux based on monthly AVHRR and ISLSCP-II data, validated at 16 FLUXNET sites. Remote Sens. Environ. 112 (3), 901–919.
Foken, T., Aubinet, M., Finnigan, J.J., Leclerc, M.Y., Mauder, M., Paw U, K.T., 2011. Results of a panel discussion about the energy balance closure correction for trace gases. Bull. Am. Meteorol. Soc. 92, ES13–ES18.
Gu, C., Ma, J., Zhu, G., Yang, H., Zhang, K., Wang, Y., Gu, C., 2018. Partitioning evapotranspiration using an optimized satellite-based ET model across biomes. Agric. For. Meteorol. 259, 355–363.
Hu, Z., Yu, G., Fu, Y., Sun, X., Li, Y., Shi, P., Wang, Y., Zheng, Z., 2008. Effects of vegetation control on ecosystem water use efficiency within and among four grassland ecosystems in China. Glob. Change Biol. 14, 1609–1619.
Huxman, T.E., Smith, M.D., Fay, P.A., Knapp, A.K., Rebecca Shaw, M., Loik, M.E., Williams, D.G., 2004. Convergence across biomes to a common rain-use efficiency. Nature 429, 651–654.
Ito, A., Inatomi, M., 2012. Water-use efficiency of the terrestrial biosphere: a model analysis focusing on interactions between the global carbon and water cycles. J. Hydrometeorol. 13, 681–694.
Keenan, T.F., Hollinger, D.Y., Bohrer, G., Dragoni, D., Munger, J.W., Schmid, H.P., Richardson, A.D., 2013. Increase in forest water use efficiency as atmospheric carbon dioxide concentrations rise. Nature 7458 (499), 324–327.
Knauer, J., Zaehle, S., Medlyn, B.E., Reichstein, M., Williams, C.A., Migliavacca, M., Linderson, M., 2018. Towards physiologically meaningful water-use efficiency estimates from eddy covariance data. Glob. Change Biol. 24, 694–710.
Lavergne, A., Graven, H., De Kauwe, M.G., Keenan, T.F., Medlyn, B.E., Prentice, I.C., 2019. Observed and modelled historical trends in the water-use efficiency of plants and ecosystems. Glob. Change Biol. 25, 2242–2257.
Law, B.E., Falge, E., Gu, L., Baldocchi, D.D., Bakwin, P., Berbigier, P., Wofsy, S., 2002. Environmental controls over carbon dioxide and water vapor exchange of terrestrial vegetation. Agric. For. Meteorol. 113, 97–120.
Li, J., Erickson, J., Peresta, G., Drake, B.G., 2010. Evapotranspiration and water use efficiency in a Chesapeake Bay wetland under carbon dioxide Enrichment. Glob. Change Biol. 16, 234–245.
Liang, W., Yang, Y., Fan, D., Guan, H., Long, D., Zhou, Y., Bai, D., 2015. Analysis of spatial and temporal patterns of net primary production and their climate controls in China from 1982 to 2010. Agri. Forest Meteorol. 204, 22–36.
Liu, X.F., Feng, X.M., Fu, B.J., 2020. Changes in global terrestrial ecosystem water use efficiency are closely related to soil moisture. Sci. Total Environ. 698, 134–165.
Manzoni, S., Vico, G., Katul, G., Fay, P.A., Polley, W., Palmroth, S., Porporato, A., 2011. Optimizing stomatal conductance for maximum carbon gain under water stress: a meta-analysis across plant functional types and climates. Funct. Ecol. 25, 456–467.
Massman, W.J., Lee, X., 2002. Eddy covariance flux corrections and uncertainties in long-term studies of carbon and energy exchanges. Agric. For. Meteorol. 113, 121–144.
McCabe, M.F., Ershadi, A., Jimenez, C., Miralles, D.G., Michel, D., Wood, E.F., 2016. The GEWEX LandFlux project: evaluation of model evaporation using tower-based and globally gridded forcing data. Geosci. Model Dev. 9 (1), 283–305.
McDowell, N., Pockman, W.T., Allen, C.D., Breshears, D.D., Cobb, N., Kolb, T., Williams, D.G., 2008. Mechanisms of plant survival and mortality during drought: why do some plants survive while others succumb to drought? New Phytol. 178, 719–739.
McDowell, N., Beerling, D.J., Breshears, D.D., Fisher, R.A., Raffa, K.F., Stitt, M., 2011. . The interdependence of mechanisms underlying climate-driven vegetation mortality. Trends in Ecology and Evolution 26, 523–532.
Medlyn, B.E., De Kauwe, M.G., Lin, Y.S., Knauer, J., Duursma, R.A., Williams, C.A., Wingate, L., 2017. How do leaf and ecosystem measures of water-use efficiency compare? New Phytol 216, 758–770.
Medrano, H., Tomás, M., Martorell, S., Flexas, J., Hernández, E., Rosselló, J., Botaa, J., 2015. From leaf to whole-plant water use efficiency (WUE) in complex canopies: Limitations of leaf WUE as a selection target. The Crop J. 220–228.
Michel, D., Jiménez, C., Miralles, D.G., Jung, M., Hirschi, M., Ershadi, A., Fernández-Prieto, D., 2016. The WACMOS-ET project–part 1: tower-scale evaluation of four remote-sensing-based evapotranspiration algorithms. Hydrol. Earth Syst. Sci. 20, 803–822.
Monteith, J.L., 1965. Evaporation and environment. Symp. Soc. Exp. Biol. 19, 205–234.
Mu, Q., Heinsch, F. A., Zhao, M., & Running, S. W. (2007). Development of a global evapotranspiration algorithm based on MODIS and global meteorology data. Remote Sensing of Environment, 111(4), 519–536. https://doi.org/10.1016/j.rse.2007.04.015.
Mu, Q., Zhao, M., Running, S.W., 2011. Improvements to a MODIS global terrestrial evapotranspiration algorithm. Remote Sens. Environ. 115 (8), 1781–1800. https://doi.org/10.1016/j.rse.2011.02.019.
Myneni, R.B., Hoffman, S., Knyazikhin, Y., Privetteb, J.L, Glassy, J., Tian, Y., Running, S. W., 2002. Global products of vegetation leaf area and fraction absorbed PAR from year one of MODIS data. Remote Sens. Environ. 83, 214–231.
Mystakidis, S., Davin, E.L., Gruber, N., Seneviratne, S.I., 2016. Constraining future terrestrial carbon cycle projections using observation-based water and carbon flux estimates. Glob. Change Biol. 22, 2198–2215.
Niu, S., Xing, X., Zhang, Z., Xia, J., Zhou, X., Song, B., Li, L., Wan, S., 2011. Water-use efficiency in response to climate change: from leaf to ecosystem in a temperate steppe. Glob. Change Biol. 17, 1073–1082.
Nossent, J., Elsen, P., Bauwens, W., 2011. Sobol' sensitivity analysis of a complex environmental model. Ecol. Model. 26 (12), 1515–1525.
Peñuelas, J., Canadell, J.G., Ogaya, R., 2011. Increased water-use efficiency during the 20th century did not translate into enhanced tree growth. Global Ecol. Biogeogr. 20, 597–608.
Penman, H.L., 1948. Natural evaporation from open water, bare soil and grass. Proc. R. Soc. Lond. A. Math. Phys. Sci. 193 (1032), 120–145.
Peters, W., van der Velde, I.R., van Schaik, E., et al., 2018. Increased water-use efficiency and reduced CO_2uptake by plants during droughts at a continental-scale. Nat Geosci 11 (9), 744–748.
Poni, S., Bernizzoni, F., Civardi, S., Gatti, M., Porro, D., Camin, F., 2009. Performance and water-use efficiency (single-leaf vs. whole-canopy) of well-watered and half-stressed split-root Lambrusco grapevines grown in Po Valley (Italy). Agric. Ecosyst. Environ. 129, 97–106.
Ponton, S., Flanagan, L.B., Alstad, K.P., Johnson, B.G., Morgenstern, K., Kljun, N., Black, T.A., Barr, A.G., 2006. Comparison of ecosystem water-use efficiency among Douglas-fir forest, aspen forest and grassland using eddy covariance and carbon isotope techniques. Glob. Change Biol. 12, 294–310.
Potts, D.L., Huxman, T.E., Cable, J.M., English, N.B., Ignace, J.A., Eilts, M.J., Williams, D. G., 2006. Antecedent moisture and seasonal precipitation influence the response of canopy-scale carbon and water exchange to rainfall pulses in a semi-arid grassland. New Phytol 170, 849–860.
Priestley, C.H.B., Taylor, R.J, 1972. On the assessment of surface heat flux and evaporation using large-scale parameters. Mon. Weather Rev. 100, 81–92.
Reichstein, M., Ciais, P., Papale, D., Valentini, R., Running, S., Viovy, N., Zhao, M., 2007. Reduction of ecosystem productivity and respiration during the European summer 2003 climate anomaly: A joint flux tower, remote sensing and modelling analysis. Glob. Change Biol. 13, 634–651.
Reichstein, M., Falge, E., Baldocchi, D., Papale, D., Aubinet, M., Berbigier, P., Valentini, R., 2005. On the separation of net ecosystem exchange into assimilation and ecosystem respiration: review and improved algorithm. Glob. Change Biol. 11, 1424–1439.
Reichstein, M., Tenhunen, J.D., Roupsard, O., Ourcival, J.M., Rambal, S., Miglietta, F., 2002. Severe drought effects on ecosystem CO_2 and H_2O fluxes at three Mediterranean evergreen sites: Revision of current hypotheses? Glob. Change Biol. 8, 999–1017.
Reichstein, M., Tenhunen, J., Roupsard, O., Ourcival, J.M., Rambal, S., Miglietta, F., Valentini, R., 2003. Inverse modeling of seasonal drought effects on canopy CO_2 H_2O exchange in three Mediterranean ecosystems. J. Geophys. Res. Atmos. 108 (D23), 4726.
Schulze, E.-D., Robichaux, R.H., Grace, J., Rundel, P.W., Ehleringer, J.R., 1987. Plant water balance: In diverse habitats, where water often is scarce, plants display a variety of mechanisms for managing this essential resource. Bioscience 37, 30–37.
Seddon, W.R., Macias-Fauria, M., Long, P.R., Benz, D., Willis, K.J., 2016. Sensitivity of global terrestrial ecosystems to climate variability. Nature (531), 229–232.

Sergio, M.V., Célia, G., Jesús, J.C., Santiago, B., Ricardo, T., Juan, I.L., Arturo, S., 2013. Response of vegetation to drought time-scales across global land biomes, 110. PNAS, pp. 52–57.
Sun, Y., Piao, S., Huang, M., Ciais, P., Zeng, Z., Cheng, L., Zeng, H., 2015. Global patterns and climate drivers of water-use efficiency in terrestrial ecosystems deduced from satellite-based datasets and carbon cycle models. Global Ecol. Biogeogr. 25, 311–323.
Tang, J., Bolstad, P.V., Ewers, B.E., Desai, A.R., Davis, K.J., Carey, E.V., 2006. Sap flux -upscaled canopy transpiration, stomatal conductance and water use efficiency on an old growth forest in the Great Lakes region of the United States. J. Geophys. Res. 111.
Tang, Q., Vivoni, E.R., Muñoz-Arriola, F., Lettenmaier, D.P., 2011. Predictability of evapotranspiration patterns using remotely-sensed vegetation dynamics during the North American monsoon. J. Hydrol. 13, 103–121.
Tarin, T., Nolan, R.H., Medlyn, B.E., Cleverly, J., Eamus, D., 2019. Water - use efficiency in a semi-arid woodland with high rainfall variability. Glob. Change Biol. 00, 1–13.
van der Molen, M.K., Dolman, A.J., Ciais, P., Eglin, T., Gobron, N., Law, B.E., Wang, G., 2011. Drought and ecosystem carbon cycling. Agric. For. Meteorol. 151, 765–773.
Wang, S.T., Zhu, G.F., Xia, D.S., et al., 2019. The characteristics of evapotranspiration and crop coefficients of an irrigated vineyard in arid Northwest China. Agric. Water Manage. 212, 388–398.
Yin, Y., Tang, Q., Wang, L., Liu, X., 2016. Risk and contributing factors of ecosystem shifts over naturally vegetated land under climate change in China. Scientific Rep 6, 20905.
Yu, G.R., Song, X., Wang, Q.F., Liu, Y.F., Guan, D.X., Yan, J.H., Wen, X.F., 2008. Water-use efficiency of forest ecosystems in eastern China and its relations to climatic variables. New Phytol 177, 927–937.
Zhang, K., Ma, J., Zhu, G., Ma, T., Han, T., Feng, L.L., 2017. Parameter sensitivity analysis and optimization for a satellite-based evapotranspiration model across multiple sites using moderate resolution imaging spectroradiometer and flux data. J. Geophys. Res. Atmos. 122, 230–245.
Zhang, Y., Peña-Arancibia, J.L., McVicar, T.R., et al., 2016. Multi-decadal trends in global terrestrial evapotranspiration and its components. Sci. Rep. 6, 19124.
Zhu, G.F., Li, X., Zhang, K., Ding, Z.Y., Han, T., Ma, J.Z., Ma, T., 2016. Multi-model ensemble prediction of terrestrial evapotranspiration across north China using Bayesian model averaging. Hydrol. Process. 30 (16), 2861–2879.